

# P11R.6 POLARIMETRIC RADAR SIGNATURES FROM RAMS MICROPHYSICS

Gwo-Jong Huang\*, V. N. Bringi, S. van den Heever and W. Cotton

Colorado State University, Fort Collins, Colorado, USA

## 1. INTRODUCTION

It is well known that dual-polarized radar can give important information on hydrometeor classification, raindrop size distribution parameters, and improved estimates of rainfall amounts. For these reasons the WSR-88D network will be upgraded for polarimetric capability within the next five years or so. A number of meteorological and hydrological agencies in Europe are actively evaluating polarimetric radar for operational applications. It is anticipated that improved algorithms will be needed for various operational products such as hydrometeor classification and rainfall estimation. High resolution 3D cloud models with sophisticated microphysical schemes can play an important role not only for providing the basis for realistic radar simulators but also for understanding the microphysical basis of the observed radar signatures, and in some sense providing for validation of polarimetric-based algorithms such as hydrometeor classifiers or rain drop size distribution estimators. In return, the radar observations can also be used to provide the basis for improved microphysical parameterizations.

The bulk microphysics version of RAMS (Walko et al 1995; Meyers et al 1997) is well-suited for coupling with a diagnostic dual-polarized radar module. The bulk microphysics is unique in that it emulates a bin-resolving model in terms of collection and sedimentation (Feingold et al. 1998; Cotton et al 2003) all within the constraints of the prescribed generalized gamma basis function. RAMS (see Cotton et al. 2003; Saleeby and Cotton, 2004) permits simulation of source/sink functions of CCN and GCCN, their activation in cloudy updrafts, and impacts on the evolution of precipitation processes. Moreover, the addition of a second cloud mode in the cloud droplet spectrum (Saleeby and Cotton 2004) provides better resolution of the collection process and permits simulation of the activation of GCCN. RAMS is now being applied to the simulation of aerosol effects on clouds and precipitation over St. Louis (van den Heever and Cotton 2005).

\*Corresponding author address: G.J. Huang, Dept. of Electrical Engineering, Colorado State University, Fort Collins, CO 80523-1373, USA.  
Email: gh222106@engr.colostate.edu

Another study of aerosol effects on clouds and precipitation is by van den Heever and Cotton (2004a) in which the effects of Saharan dust on Florida convection were explored. That study showed that Saharan dust greatly altered the dynamics of the storms as well as convective rainfall amounts.

Simulations of deep convective storms (e.g., supercells) have also shown the importance of microphysical processes in modulating, for example, storm structure, cold pool dynamics, the distribution of precipitation with respect to the updraft and the low level velocity (e.g., van den Heever and Cotton 2004b; Gilmore et al 2004; Saleeby and Cotton 2004). On the other hand, dual-polarized radar signatures in deep convection can be used to infer certain 'bulk' microphysical features such as, for example, warm rain development, coalescence-freezing, wet growth of hail aloft, shedding by large wet hail, development of the precipitation balance level, etc (Illingworth et al 1987; Wakimoto and Bringi 1988; Tuttle et al 1989; Herzegh and Jameson 1992; Conway and Zrnić 1993; Hubbert et al 1998; Smith et al 1999; Zeng et al 2001; Loney et al 2002). The coordinated analyses of polarimetric radar storm 'structure', and cloud model simulations should provide important new linkages between storm microphysics and dynamical evolution that may not be separately evident.

In this paper we present some preliminary examples of the expected polarimetric radar signatures based on some of the RAMS microphysical outputs for simulations already reported by van den Heever and Cotton (2004a,b; 2005). The radar simulations are performed using the T-matrix scattering code at each grid point using the RAMS predicted mixing ratio and number concentration along with suitable assumptions on particle shape, orientation and dielectric constant.

## 2. DROP SIZE DISTRIBUTION VARIABILITY

We first consider drop size distribution variability in terms of the two parameters, (a) the mass-weighted mean diameter ( $D_m$ ) and (b) the normalized intercept parameter ( $N_w$ ) of a gamma dsd (similar to  $N_0$  of the exponential dsd). Both parameters can be accurately retrieved from polarimetric radar measurements of  $Z_{dr}$ ,  $Z_{dp}$ .

Fig. 1 shows a plot of  $\log_{10}\langle N_w \rangle$  versus  $\langle D_m \rangle$  for convective rain (with  $R > 5$  mm/h) where angle brackets represent long-term time averages (for disdrometer data) and spatial averages for radar based retrievals (details can be found in Bringi et al

2003). From Fig. 1 a "maritime" cluster with  $\langle D_m \rangle$  in the range 1.5 to 1.75 mm and  $\log_{10} \langle N_w \rangle$  from 4-4.5 (note the units of  $N_w$  in  $\text{mm}^{-1} \text{m}^{-3}$ ; for reference the Marshall-Palmer  $N_w$  is 8000) can be noted. The Fort Collins flash flood storm of 1997 is unusual for Colorado as the data fall in the maritime cluster (this was independently confirmed by Petersen et al 1999).

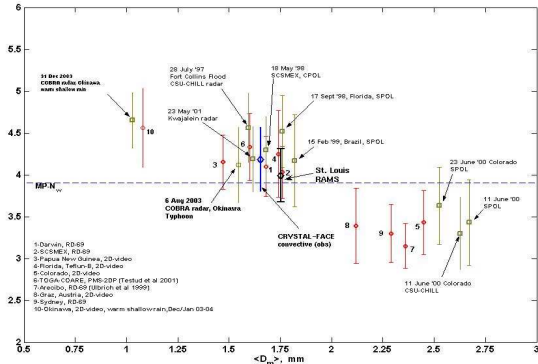


Fig. 1:  $\log_{10} \langle N_w \rangle$  and  $\pm 1\sigma$  versus  $\langle D_m \rangle$  from disdrometer, radar retrievals and RAMS simulations. Angle brackets refer to average values for  $R > 5 \text{ mm/h}$  in convective rain. 'CRYSTAL-FACE' simulations are based on observed values of CCN and GCCN in Florida. 'St Louis RAMS' refers to simulations using CCN and GCCN released from urban area (St Louis). Note: MP- $N_w$  refers to Marshall Palmer value of  $8000 \text{ mm}^{-1} \text{m}^{-3}$ .

In order to see where RAMS 2-moment simulations of the average rain dsd would lie in Fig. 1, we took the case from van den Heever and Cotton (2004a) who simulated the high aerosol concentrations (Saharan dust) observed during CRYSTAL-FACE. The 2-moment scheme for rain gave  $\langle D_m \rangle$  and  $\log_{10} \langle N_w \rangle$  as plotted in Fig. 1 for their experiment with 'observed' CCN and GCCN concentrations (i.e., high aerosol concentration case). The average dsd parameters were taken from the mature evolution stage of the simulations. Note how the averaged dsd parameters fall within the maritime cluster. We found no significant differences in the average dsd parameter values when we used their 'clean' CCN and GCCN runs (i.e., normal background aerosol concentrations).

From Fig. 1 a "continental" cluster can also be identified which is characterized by larger  $\langle D_m \rangle$  from 2-2.75 mm and smaller  $\log_{10} \langle N_w \rangle$  from 3-3.5. Li et al (2003) have used a 2D bin spectral model to simulate the effects of 'clean' versus 'polluted' CCN on the Z-R relation in the rain layer of a tropical convective system during TOGA-COARE. At the 3.1 km height they deduced a 'clean'  $Z=287R^{1.74}$  relation whereas the 'polluted' relation was  $Z=514R^{1.6}$ . They inferred that "...polluted air produces rain that has larger mean diameters" than 'clean' air. In essence, their 'clean' case would on average fall near the maritime cluster

in Fig. 1, whereas their 'polluted' case would fall within the continental cluster. We were not able to observe such a clear distinction in the 'clean' and 'observed' simulations of van den Heever and Cotton (2004a) perhaps because they included both CCN and GCCN in both runs (albeit with reduced concentrations of GCCN for the 'clean' run). While it is known that enhanced CCN concentrations will tend to suppress warm rain processes, the presence of GCCN (even at background levels) would tend to support warm rain processes. This may be the reason for the discrepancy alluded to above.

To illustrate the dependence of  $D_o$  and  $N_w$  versus  $R$ , Fig. 2 shows SPOL radar-based retrievals from the 17 September 1998 event (during TEFLUN-B in Florida) compared with 2D video disdrometer data (operated by University of Iowa) from all convective events over a 2 month period (details are provided in Bringi et al 2003). Fig. 2 shows that the radar retrievals are not only reasonable (in terms of variability) when compared with 2D video data but, in addition, very few of the disdrometer data points lie outside the radar-derived "envelope" of  $D_o$  (which is close to  $D_m$ ) and  $N_w$ . At high rain rates, the radar and disdrometer  $D_o$  values tend to a stable value around 1.7-2 mm, reflecting the tendency for equilibrium-like distributions where drop breakup and coalescence are in near balance (e.g., Hu and Srivastava 1995; Uijlenhoet et al 2003). Steiner et al (2004) refer to this equilibrium as a special microphysical condition where all variability in the dsd is controlled by variations in number concentration leading to a linear Z-R relation (as opposed to the other extreme of being "size controlled"). In general, the dsd is controlled by a "mix" of variations in  $N_i$  and  $D_o$  (e.g., at low-to-moderate  $R$  in Fig 2).

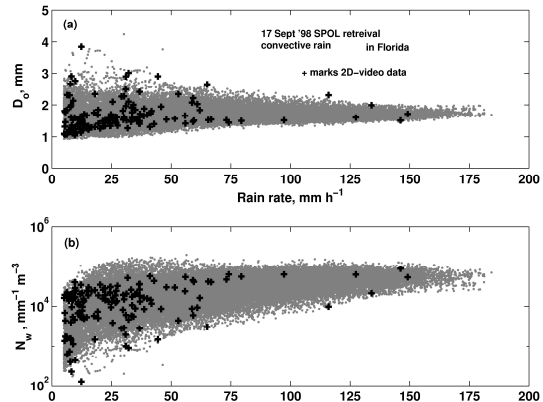


Fig. 2:  $D_o$  and  $N_w$  versus rain rate from SPOL radar retrievals from the 17 September 1998 event. The '+' marks are from 2D video disdrometer data from all convective rain events during the 1998 TEFLUN experiment.

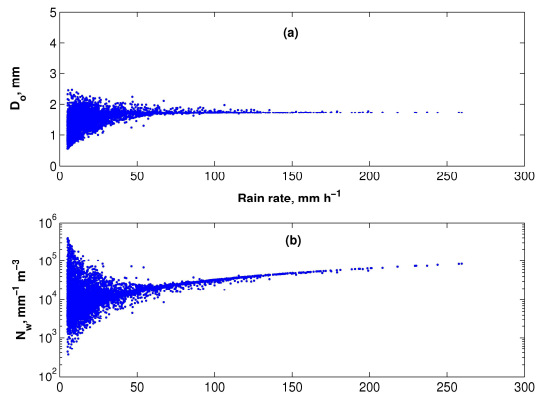


Fig. 3: Scatter plot of (a)  $D_0$  and (b)  $N_w$  versus rain rate from RAMS 2-moment simulations from CRYSTAL-FACE in Florida (van den Heever and Cotton 2004a).

Fig. 3 shows similar scatter plots for convective rain based on the RAMS 2-moment simulations (with  $\mu$  fixed at 1) including the effects of Saharan dust on Florida thunderstorms (van den Heever and Cotton 2004a). Note the general similarity with Fig. 2 especially at high rain rates. Note also the much reduced range of variability in the simulated data as compared with the radar retrievals and the disdrometer data (this may be due to fixing the shape of the gamma dsd in the simulations with  $\mu$  preset at 1). At least for higher  $R$ , the behavior of  $N_w$  and  $D_m$  are consistent between the RAMS 2-moment scheme and the radar-based retrievals shown in Fig.2 (only the observed CCN/GCCN case is shown in Fig 3, van den Heever and Cotton 2004a). This agreement between observations and model predictions is very encouraging.

### 3. SUPERCELL SIMULATION

van den Heever and Cotton (2005) studied the sensitivity of simulated supercell storms to varying the mean mass diameter of the hail size distribution from 3 mm to 1 cm using the single moment scheme of RAMS assuming exponential shape. They found that with smaller hailstones, for example, low level downdrafts were stronger and the cold pools were deeper and more intense due to increased rate of cooling due to hail melting and evaporation of water off the hail surface, in agreement with the work of Srivastava (1987). Here we simulate  $Z_h$ ,  $Z_{dr}$ ,  $K_{dp}$  and LDR for the 3 mm hail simulation using only the predicted rain and hail mixing ratios from the RAMS output. To obtain realistic  $Z_{dr}$  values in rain, we assumed that the intercept parameter is fixed at  $N_0=8000 \text{ mm}^{-1} \text{ m}^{-3}$  i.e., the Marshall-Palmer intercept value, and derived the mean mass diameter from the rain mixing ratio (as otherwise  $Z_{dr}$  would be constant everywhere in the rain). Raindrops are assumed to be oblate with the equilibrium axis ratios given by Beard and Chuang. The canting angle is assumed to be

Gaussian in shape with standard deviation of  $5^\circ$ . For the hailstones, we derived the intercept value using the RAMS predicted hail mixing ratio and assuming the mean mass diameter is 3 mm. The hailstones are assumed to be oblate with axis ratio= 0.8 with random orientation. Below 5.2 km height, the hail is assumed to be wet (50% water/50% ice mixture). Higher than 5.2 km the hail is assumed to be 'dry'.

Fig. 4 shows the vertical cross section (east-to-west) at 60 minutes into the simulation. Low-level flow enters the storm from the south and east and rises in the updraft. Mid-level air enters the updraft from the south and the updraft diverges at the tropopause level. Peak updrafts at mid levels exceeded 50 m/s. The 4 panels of Fig. 5 show the simulated  $Z_h$ ,  $Z_{dr}$ , LDR and  $K_{dp}$  fields. The positive  $Z_{dr}$  column is clearly visible at 64 km distance extending from 4-6 km in height.

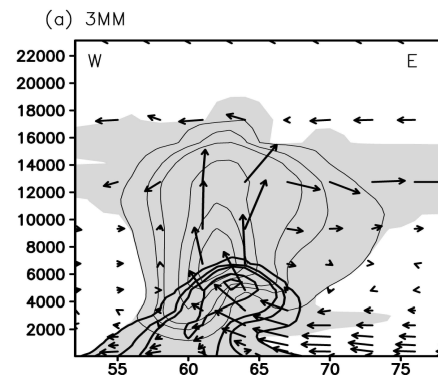
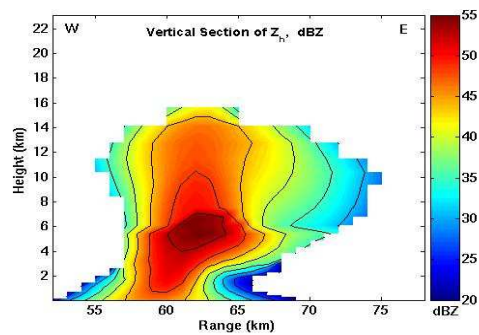


Fig. 4: Vertical cross section of the supercell simulation at 60 minutes. Shading indicates regions where condensate mixing ratio  $> 0.1 \text{ g/kg}$ . Hail mixing ratios are in thin lines and rain mixing ratio in thick lines. Contours are at 0.1, 0.5, and then from 1 to max value in steps of 2 g/kg. From van den Heever and Cotton (2004b).



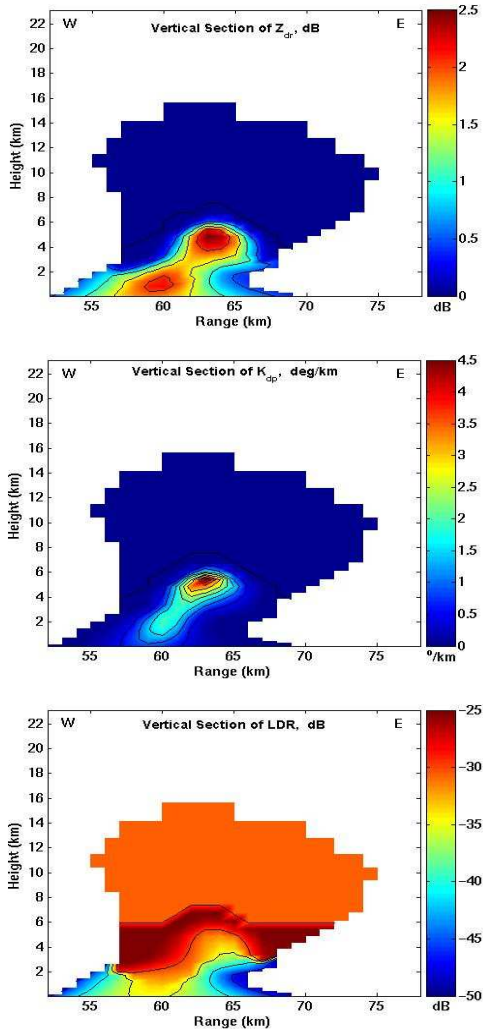


Fig. 5: Vertical cross sections of radar observables from single moment RAMS supercell simulation. Radar simulations use only the rain and hail output of RAMS.

Such columns have been noted in previous observations of (high precipitation) supercells (e.g., Hubbert et al 1998; Conway and Zrnić 1993; Loney et al 2002). The LDR simulations show an enhanced LDR 'cap' signature (due to wet hail) on top of the positive  $Z_{dr}$  column which has been observed by Hubbert and Bringi (1998). The  $K_{dp}$  simulations show a clear region of high rain water content at 5.5-6 km height (independent of the hail content there). Typically, the descent of this high  $K_{dp}$  region is often related to descent of the main precipitation core and the formation of strong downdrafts. There is some evidence that forecasters, supplied with the prototype dual-polarized WSR-88D data, have used the persistence of positive  $Z_{dr}$  columns extending above the  $0^{\circ}$  C level, as added information of storm severity

(Scharfenberg et al 2003). With the advent of polarimetric capability for the WSR-88D radars in the next five years, it would be important to be able to identify such signatures in real-time and be able to track them for indications of storm severity.

#### 4. URBAN HEAT ISLAND

There is considerable evidence that major urban areas cause increased occurrences of severe weather and lightning. However, the causes of observed precipitation and severe weather anomalies over and downwind of urban areas are still not well understood. RAMS has already been used to simulate the urban heat island over St. Louis (Rozoff et al. 2003). The Town Energy Budget (TEB) model has now been interfaced with the aerosol version of RAMS microphysics within which the concentrations of CCN, GCCN and IFN are prognostic variables and permit simulation of sources and sinks of CCN and GCCN, Saleeby and Cotton (2004).

The simulation of aerosol affects on clouds and precipitation over St. Louis is under investigation (van den Heever and Cotton 2005). We consider the RAMS simulations from this latter work using one of their sensitivity runs, termed as 'URBAN' where CCN and GCCN are continuously released from the urban St. Louis region. The surrounding rural areas have their background CCN/GCCN values. The RAMS 2-moment scheme with gamma shape ( $\mu=v-1=1$ ) was used for all species; we consider here only the rain, hail, graupel and snow. From the RAMS predicted number concentration and mixing ratio we deduce the normalized intercept parameter ( $N_w$ ) and the mass-weighted mean diameter ( $D_m$ ) for each species. The rain and hail shape/orientation are modeled as before for the supercell case. The graupel is assumed to be oblate (axis ratio of 0.8) with random orientation. Below  $0^{\circ}$  C they are 'dry' with density=0.55 g/cc; at levels warmer than  $0^{\circ}$  C they are assumed to be 'wet' with 35% water, 35% ice and 30% air mixture. The snow is assumed to oblate with axis ratio of 0.2 ('disk'-like), density of 0.23 g/cc and with Gaussian canting angle distribution with mean 0 and standard deviation of  $40^{\circ}$ . As modeled, they will give rise to positive  $Z_{dr}$  values aloft. The RAMS simulations clearly showed the development of the urban heat island over St. Louis. Cumulus convection started to form SW of the city around 1800 UTC and by 1900 UTC deep moist convection developed. Here we show one 'snap shot' of the convection at 2115 UTC depicted in Fig. 6 with reflectivity contours at 4 km height. The storm NW of St. Louis is downwind of the city with corresponding advection of CCN and GCCN into that area. A vertical section of the various mixing ratios of rain, hail, graupel and snow are shown in Fig. 7 along the E-W line marked in Fig. 6. Fig. 8 shows four panels of vertical sections along the same E-W line of  $Z_h$ ,  $Z_{dr}$ ,  $K_{dp}$  and LDR. Notable features are as follows.

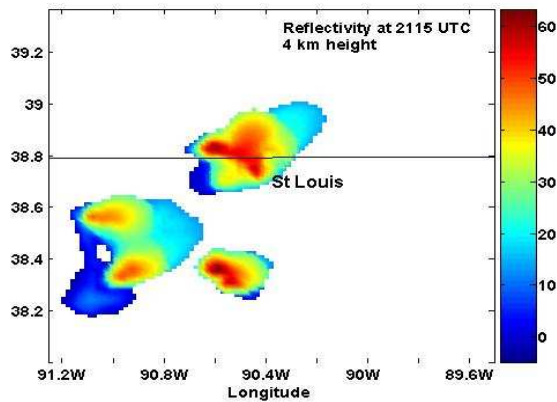


Fig. 6: Radar simulated reflectivity at 4 km height at 2115 UTC. Vertical sections are presented along the horizontal line (east-west) in Figs. 7 and 8 below.

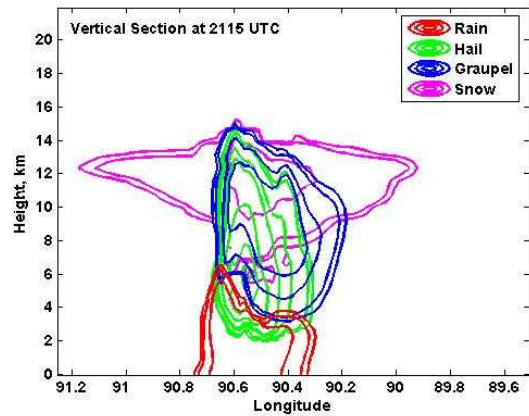
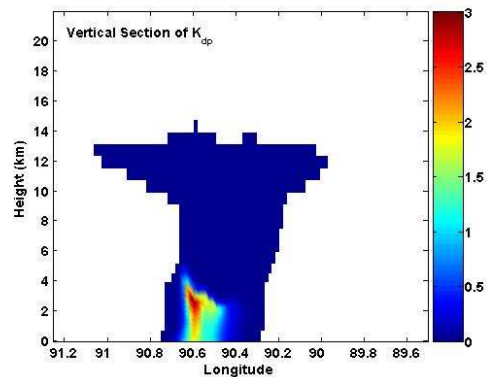
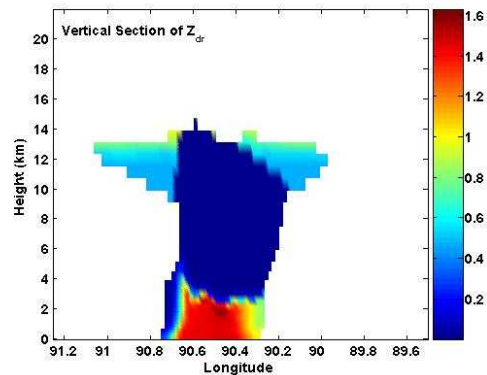
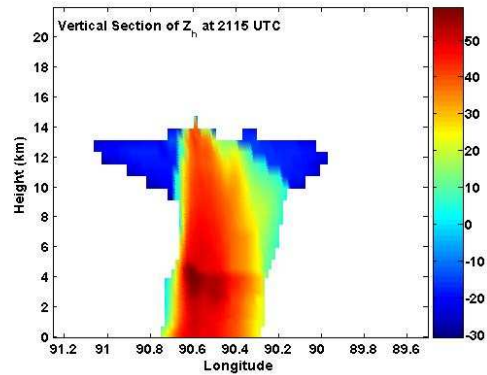


Fig. 7: Vertical section from RAMS output of rain, hail, graupel and snow mixing ratios. Contours are at 0.05 g/kg, 0.1, 0.5, and then from 1 to max value in steps of 2 g/kg.

From Fig. 7, hail descends to 2 km height, well below the 0 C level before complete melting into rain. There is a mid-level updraft on the eastern side of the storm which fails to produce a strong positive  $Z_{dr}$  column. The 'melting' level from  $Z_{dr}$  is inferred to be at 3 km height well below the 0 C level, again because of hail. The  $K_{dp}$  data shows enhanced rain water contents closer to the eastern edge with the maximum values near 3 km height. There is a hint of a positive  $K_{dp}$  column reaching at most 4 km height. The LDR data shows enhancement due to wet hail between 2 and 4 km height. With this much hail melt contributing to the rain, it was expected that the mass-weighted mean diameter ( $D_m$ ) would have been large with correspondingly lower  $N_w$  values falling within the continental cluster in Fig. 1. However, the average values of  $D_m$  and  $N_w$  from the 1 km height (for  $R > 5$  mm/h) place it within the maritime cluster in Fig. 1 with

$\langle D_m \rangle = 1.75$  mm and  $N_w = 10,000$  mm<sup>-1</sup> m<sup>-3</sup>. The microphysical reasons for this are under investigation.



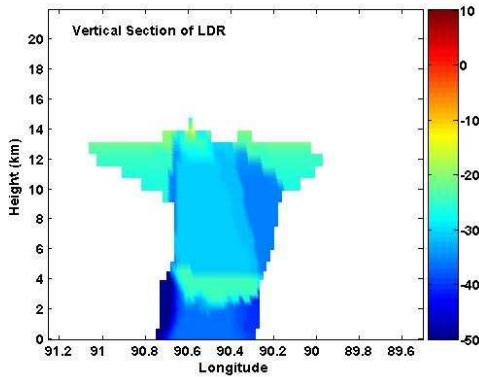


Fig. 8: Four panels show vertical cross sections of  $Z_h$ ,  $Z_{dr}$ ,  $K_{dp}$  and LDR at 2115.

Finally, we show the scatter plot of DSD parameters  $D_0$  and  $N_w$  versus rain rate in Fig. 9 which may be compared with Fig. 3 (the CRYSTAL-FACE simulations) and with Fig. 2 based on radar retrievals and disdrometer data. Again, the  $D_0$  tends to a steady value near 1.8-2 mm as  $R$  increases which is consistent with equilibrium distributions.

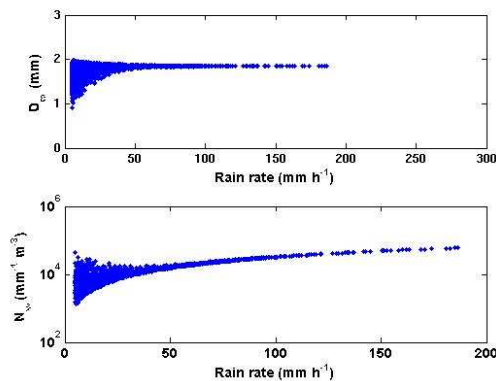


Fig. 9: Scatter plots of  $D_m$  (top panel) and  $N_w$  (bottom panel) versus rain rate from the RAMS St Louis Urban simulation. Data from height of 907 m with  $R > 5$  mm/h.

ACKNOWLEDGEMENTS: Two of the authors (VNB and GJH) acknowledge support from the National Science Foundation via grant ATM-9982030. vdH and WC acknowledge support from ATM-9900929.

## REFERENCES

Beard, K.V. and C. Chuang, 1987: A new model for the equilibrium shape of raindrops, *J. Atmos. Sci.*, vol. 2, 468-471.

Bringi, V.N., V. Chandrasekar, J. Hubbert, E. Gorgucci, W.L. Randeu and M. Schoenhuber, 2003: Raindrop size distribution in different climatic

regimes from disdrometer and dual-polarized radar analysis, *J. Atmos. Sci.*, vol. 60, 354-365.

Conway, J.W. and D.S. Zrnić, 1993: A study of embryo production and hail growth using dual-Doppler and multiparameter radars, *Monthly Weather Review*, vol. 121, 2511-2528.

Cotton, W.R., R.A. Pielke, Sr., R.L. Walko, G.E. Liston, C.J. Tremback, H. Jiang, R.L. McAnelly, J.Y. Harrington, M.E. Nicholls, G.G. Carrió, J.P. McFadden, 2003: RAMS 2001: Current status and future directions, *Meteor. Atmos. Physics*, vol. 82, 5-29.

Feingold, G., R.L. Walko, B. Stevens and W.R. Cotton, 1998: Simulations of marine stratocumulus using a new microphysical parameterization scheme, *Atmos. Res.*, vol. 47-48, 505-528.

Gilmore, M.S., J.M. Straka and E.N. Rasmussen, 2004: Precipitation and evolution sensitivity in simulated deep convective storms: Comparisons between liquid-only and simple ice and liquid phase microphysics, *Monthly Weather Review*, vol. 132, 1897-1916.

Herzogh, P.H. and A.R. Jameson, 1992: Observing precipitation through dual-polarization radar measurements, *Bull. Amer. Meteor. Soc.*, vol. 73, 1365-1374.

Hu, Z. and R.C. Srivastava, 1995: Evolution of raindrop size distribution by coalescence, breakup and evaporation: Theory and observations, *J. Atmos. Sci.*, vol. 52, 1781-1783.

Hubbert, J., V.N. Bringi, L.D. Carey and S. Bolen, 1998: CSU-CHILL polarimetric radar measurements in a severe hailstorm in eastern Colorado, vol. 37, 749-775.

Illingworth, A.J., J.W.F. Goddard and S.M. Cherry, 1987: Polarization radar studies of precipitation development in convective storm, *Q. J. Roy. Meteor. Soc.*, vol. 113, 469-489.

Li, X., W. Tao, J. Simpson, A. Khain and D. Johnson, 2003: Radar reflectivity simulated by a 2-D spectral bin model and its sensitivity on cloud-aerosol interaction, *31st Int. Conf. on Radar Meteor.*, Seattle, Amer. Meteor. Soc., 39-43.

Meyers, M.P., R.L. Walko, J.Y. Harrington and W.R. Cotton, 1997: New RAMS cloud microphysics parameterization. Part II: The two-moment scheme, *Atmos. Res.*, vol. 45, 3-39.

Rozoff, C.M., W.R. Cotton and J.O. Adegoke, 2003: Simulation of St. Louis, Missouri, Land Use Impacts on Thunderstorms, *J. Appl. Meteor.*, vol. 42, 716-738.

Saleeby, S.M. and W.R. Cotton, 2004: A large-droplet mode and prognostic number concentration of cloud droplets in the Colorado State University Regional Atmospheric Modeling System (RAMS). Part I: Module descriptions and supercell test simulations, *J. Appl. Meteor.*, vol. 43, 182-195.

Scharfenberg, K.A., D.L. Jr. Andra and M.P. Foster, 2003: Operational uses of polarimetric radar data in severe local storm prediction, *31st Int. Conf. on Radar Meteor.*, Seattle, Amer. Meteor. Soc., 632-634.

Smith, P.L., D.J. Musil, A.G. Detwiler and R. Ramachandran. 1999: Observations of mixed-phase precipitation within a CaPE thunderstorm, *J. Appl. Meteor.*, vol. 38, 145-155.

Srivastava. R.C., 1987: A model of intense downdrafts driven by the melting and evaporation of precipitation, *J. Atmos. Sci.*, vol. 44, 1752-1773.

Tuttle, J.D., V.N. Bringi, H.D. Orville and F.J. Kopp, 1989: Multiparameter radar study of a microburst: Comparison with model results, *J. Atmos. Sci.*, vol. 46, 601-620.

Uijlenhoet, R., J.A. Smith and M. Steiner, 2003: The microphysical structure of extreme precipitation as inferred from ground-based raindrop spectra, *J. Atmos. Sci.*, vol. 60, 1220-1238.

van den Heever, S.C. and W.R. Cotton, 2004a: The impacts of Saharan dust on Florida convection, *Proc. 14th Int. Conf. Clds. Precip.*, Bologna, Italy, 18-23 July.

van den Heever, S.C., and W.R. Cotton, 2004b: The impact of hail size on simulated supercell storms, *J. Atmos. Sci.*, vol. 61, 1596-1609.

van den Heever, S.C., and W.R. Cotton, 2005: Modeling the impacts of urban aerosol on convection and precipitation, *16th Conference on Planned and Inadvertent Weather Modification*, AMS, San Diego, CA.

Wakimoto, R.M. and V.N. Bringi, 1988: Dual-polarization observations of microbursts associated with intense convection: The 20 July storm during the MIST project, *Monthly Weather Review*, vol. 116, 1521-1539.

Walko, R.L., W.R. Cotton, M.P. Meyers and J.Y. Harrington, 1995: New RAMS cloud microphysics parameterization. Part I: The single-moment scheme, *Atmos. Res.*, vol. 38, 29-62.

Zeng, Z., S.E. Yuter, R.A. Houze Jr. and D.E. Kingsmill, 2001: Microphysics of the rapid development of heavy convective precipitation, *Monthly Weather Review*, vol. 129, 1882-1904.